# Stiffness-constant variation in nickel-based alloys: Experiment and theory

M. Hennion and B. Hennion

*Commissariat a l'Energie Atomique, Division de la Physique, Service de Physique du Solide et de Resonance Magnetique, Boite Postale No. 2, 91190 Gif Sur Yvette, France*

(Received 22 June 1978)

Recent measurements of the spin-wave stiffness constant in several nickel alloys at various concentrations are interpreted within a random-phase approximation, coherent-potential approximation (RPA-CPA) band model which uses the Hartree-Fock approximation to treat the intraatomic correlations. We give a theoretical description of the possible impurity states in the Hartree-Fock approximation. This allows the determination of the Hartree-Fock solutions which can account for the stiffness-constant behavior and the magnetic moment on the impurity for all the investigated alloys. For alloys such as *Ni*Cr, *Ni*V, *Ni*Mo, and *Ni*Ru the magnetizations of which deviate from the Slater-Pauling curve, our determination does not correspond to previous works and is consequently discussed. The limits of the model appear mainly due to local-environment effects; in the case of *Ni*Mn, it is found that a ternary-alloy model with some Mn atoms in the antiferromagnetic state can account for both stiffness-constant and magnetization behaviors.

## I. INTRODUCTION

The electronic structure of transition-metal alloys has been fairly well investigated either by measurements of mean properties such as magnetization, resistivity, and specific heat or by measurements of local properties obtained by diffuse neutron scattering such as the magnetic moment on the impurity and the extension of the perturbation. In the case of nickel alloys, these various measurements enable one to distinguish between two classes of alloys according to whether their magnetizations follow the Slater-Pauling curve or not. Many theoretical models have been developed to account for these properties by using the Slater-Koster theory with a Hartree-Fock scattering potential. For instance, the models of Campbell and Gomes[1] and of Demangeat and Gautier[2] may account for the different magnetization behaviors with the assumption that the impurity has one of two different electronic states, possible solutions of the Hartree-Fock equations. These models support Friedel's concept[3] of a virtual bound state in order to explain the important modification of the magnetic properties when the impurity has a very different valency from the host. Such a study has also been extended to concentrated alloys by combining the Hartree-Fock approximation and the tight-binding model with the use of the coherent-potential approximation (CPA).[4] More recently, several authors[5,6] have reported the variation of the magnetic moment of the impurity with the atomic number for all the solutions of the Hartree-Fock equation. Hayakawa and Yamashita[5] have discussed the capability of this model to describe some magnetic properties of dilute alloys.

In these works, attention was mostly focused on the mean magnetization and the magnetic moment of the impurity, and in some cases the specific heat[4] or the residual resistivity.[5]

We intend here to extend the analysis to the stiffness-constant variations of these alloys. Indeed, measurements of the $D$ constant have been performed by inelastic neutron scattering in several nickel alloys at various concentrations, and reported in previous papers.[7-10,37,38] They show that, regardless of the magnetic behavior, the stiffness constant $D$ decreases with concentration in all the investigated alloys. However, the decrease has different characteristics depending on the class of the alloy. For *Ni*Co, *Ni*Fe, and *Ni*Mn, the decrease is more pronounced at small concentration and more so as the excess of charge $Z$ in the matrix increases (from Co to Mn). For *Ni*Cr, *Ni*V, *Ni*Ru, and *Ni*Mo, $D$ decreases linearly with concentration and follows the magnetization curve with, however, a little deviation from the linearity in the *Ni*Ru case. The close relation between the stiffness constant and the band structure of electrons is now well established, and several theoretical models[11-14] allow the calculation of its variation in concentrated alloys by using the CPA. Of course, these calculations use further approximations compared to the models developed for the pure-metal case. For instance, it is necessary to use a rigid-band splitting $\Delta$, a momentum-independent intra-atomic constant $U$, equivalent $d$ subbands, the classical RPA, etc. It is then of interest to check the limits of validity of such models.

The purpose of this paper is to examine (i) the capability of the RPA-CPA model of giving a general interpretation of the stiffness constant together with magnetization variations of Ni alloys (Sec. II) and (ii) the limits of the model for each class of alloys (Sec. III), within our approximations.

## II. HARTREE-FOCK SOLUTIONS

### A. Model

The stiffness constant of the alloys is interpreted within the model of Riedinger and Nauciel-Bloch.[13,14] Since it has already been described, we only recall briefly the main equations.

As did Hasegawa and Kanamori,[4] we adopt the tight-binding Hamiltonian with the "$d$" electrons only. Within the equivalent-orbital description, the "atomic" energies of electrons are expressed in the Hartree-Fock approximation by

$$\epsilon_{\alpha,\sigma}=\epsilon_{\alpha 0}+4(U_\alpha-J_\alpha)N_{\alpha\sigma}+5U_\alpha N_{\alpha-\sigma}\,,$$
$$\alpha=A,B,\quad \sigma=\uparrow,\downarrow\,,$$

where the intra-atomic constants $U$ and $J$ are, respectively, the Coulomb and exchange interaction parameters.

Calculation at any concentration can be made by using the coherent-potential theory[15,16] in which is defined an effective uniform medium characterized by the self-energy $\Sigma_\sigma(z)$.

The Green's function $F_{\alpha,\sigma}$ of the $\alpha$ atom in the effective uniform medium is related to the Green's function $F_\sigma(z)$ of this medium through the Dyson equation which yields the relation

$$F_{\alpha,\sigma}(z)=F_\sigma(z)/\{1-[\epsilon_{\alpha,\sigma}-\Sigma_\sigma(z)]F_\sigma(z)\}\,, \tag{1}$$

with $F_\sigma(z)$ related to the Green's function of the pure medium $F^0(z)$ by

$$F_\sigma(z)=F^0[z-\Sigma_\sigma(z)]=\int\frac{n^0(E)}{z-\Sigma_\sigma(z)-E}\,dE\,,$$

where $\Sigma_\sigma(z)$ is given by the implicit equation

$$\sum_\alpha x_\alpha\frac{\epsilon_{\alpha,\sigma}-\Sigma_\sigma(z)}{1-[\epsilon_{\alpha,\sigma}-\Sigma_\sigma(z)]F_\sigma(z)}=0\,, \tag{2}$$

which expresses statistically that an electron propagating in the effective medium is not scattered.

Solving simultaneously the set of implicit equations (1) and (2), we get $\Sigma_\sigma(z)$ and $F_\sigma(z)$, and then the number of electrons for each site,

$$N_{\alpha,\sigma}=-\frac{1}{\pi}\,\mathrm{Im}\int_{-\infty}^{E_F}F_{\alpha,\sigma}(z)\,dz\,,$$

where the Fermi energy is obtained from the condition of conservation of the total number of electrons:

$$N^0(x)=\sum_{\alpha,\sigma}N_{\alpha,\sigma}\,.$$

The $N_{\alpha,\sigma}$ and $E_F$ parameters are determined self-consistently by a minimization method[17] (see Appendix).

Once $\Sigma_\sigma(z)$ is calculated, the stiffness constant $D$ is derived through the analytical expression of Riedinger and Nauciel-Bloch:[14]

$$D=-\frac{1}{3\pi m}\,\mathrm{Im}\int_{-\infty}^{E_F}dE\{\tfrac{1}{2}[\mathfrak{M}'(E^+-\Sigma_\uparrow(E^+))+\mathfrak{M}'(E^+-\Sigma_\downarrow(E^+))]-[\Sigma_\downarrow(E^+)-\Sigma_\uparrow(E^+)]^{-1}$$
$$\times[\mathfrak{M}(E^+-\Sigma_\uparrow(E^+))-\mathfrak{M}(E^+-\Sigma_\downarrow(E^+))]\}\,,\quad E^+=E+i\epsilon\,,$$

which uses the random-phase approximation. An equivalent expression has been derived by Fukuyama[11] and Hill and Edwards.[12] In this formula, $\mathfrak{M}(z)$ is given by

$$\mathfrak{M}(z)=\int_{-\infty}^{+\infty}\frac{M(E)}{z-E}\,dE\,,$$

which is the analytical extension of the $M(E)$ function introduced by Wakoh,[18]

$$M(E)=\int_{S(E)}\nabla_k E(k)\,dS\,.$$

### B. Parameters

We have used the parametrization of the functions $n^0(E)$ and $M(E)$ of pure nickel given by Riedinger and Nauciel-Bloch[14] corresponding to the band-structure calculation of Fletcher[19] with a bandwidth $W=0.32$ Ry (4 eV).

Besides the density of states, for each alloy two sets of parameters are needed: $U_\alpha+4J_\alpha=U_\alpha^{\mathrm{eff}}$ and $\delta_0=\epsilon_{B0}-\epsilon_{A0}$, which are kept constant at all concentrations. All the others are evaluated consistently. The value of $U^{\mathrm{eff}}$ for pure nickel and therefrom the splitting value $\Delta=U^{\mathrm{eff}}m$ has been determined by fitting the calculated $D$ constant to the experimental value ($D\simeq 540$ MeV Å$^2$)[7,20] which yields $U^{\mathrm{eff}}=0.5$ Ry or $\Delta=0.06$ Ry. As already said in previous papers,[21] this $\Delta$ value stands at the maximum edge of the range of values obtained in band-structure calculations ($0.027<\Delta<0.07$ Ry)[22-26] and, therefore, is rather large. This procedure has, nevertheless, been chosen because of the sensitivity of the constant $D$, on one hand to the $U^{\mathrm{eff}}$ or $\Delta$ value (indeed $D$ increases down to 260 meV Å$^2$ when $\Delta=0.03$ Ry), and on the other hand to the approximations of the model (the experimental $D$ value of pure nickel may be well ac-

counted for in the more elaborate model of Cooke and Davis,[27] which uses the mean splitting value $\Delta = 0.027$ Ry from the calculation of Hodges *et al.*[23]).

Accordingly, the parameter $U^{\text{eff}}$ has to be considered an effective parameter of the model, and we do not have to draw physical conclusions on the band structure from its large value. For instance, this may be responsible for too large deformations in the band structures, but that error has only little effect on the mean magnetization or the magnetic moment on the impurity obtained by a simple integration over the band. As to the stiffness constant, the comparison between calculation and experiment is thought to be meaningful as far as it is extended to several alloys.

The $U^{\text{eff}}$ value for impurities of the first transition series has been determined so that the ratio $U_{\text{Ni}}/U_B$ ($B$ is the impurity) approximately corresponds to the theoretical calculations of Fletcher and Nudel.[28] A similar variation has been used for impurities of the second transition series (cf. Fig. 1). The decrease of this parameter corresponds to the extension of the electronic orbital of isolated atoms. The sensitivity of the calculation to a change in this ratio may be appreciated by comparing results of *Ni*Cr and *Ni*Mo in Fig. 10. The results are similar, although the $U_B^{\text{eff}}$ value changes by 30%. (The other parameters have the same value since these alloys are isoelectronic.)

The parameter $\delta_0 = \epsilon_{B0} - \epsilon_{A0}$ affects more the results, and its determination is somewhat difficult. We have chosen to determine it starting from the calculation of the energy difference $\delta = \epsilon_B - \epsilon_A$ of the isolated atom in the paramagnetic state and using the relation

$$\delta = \delta_0 + \tfrac{1}{2}(9U_B - 4J_B)\, n_{0B} - \tfrac{1}{2}(9U_A - 4J_A)\, n_{0A},$$

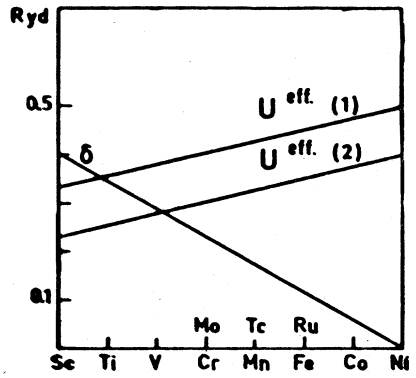


FIG. 1. Variation of the effective intra-atomic parameter $U^{\text{eff}}$ and of the parameter $\delta = \epsilon_B - \epsilon_{\text{Ni}}$ in the paramagnetic state as a function of the impurity. The lines $U(1)$ and $U(2)$ correspond to the $U^{\text{eff}}$ variation of atoms in the first and second transition series.

where $n_{0A}$ and $n_{0B}$ are the numbers of electrons of pure metals in the paramagnetic state. According to the calculation of Herman and Skillman[29] on the isolated atoms, $\delta$ follows a linear variation with $Z$ providing a change of 0.8 eV for $\Delta Z = 1$. It is clear that this determination which refers to a calculation on isolated atoms and requires an extra equation is rather approximate. It has been, nevertheless, adopted for the weak ferromagnetic alloys, since it yields reasonable critical concentrations. The sensitivity of the results to the $\delta$ value is shown in Fig. 11 in the case of *Ni*Ru.

For the strong ferromagnets, the same procedure provides too large a magnetic moment on the impurity (~1.9 $\mu_B$, 3.4 $\mu_B$, and 4.2 $\mu_B$ on Co, Fe, and Mn, respectively). But in these alloys the determination of $\delta_0$ is facilitated by the fact that the magnetic moment is very sensitive to this parameter. Since the experimental values of the magnetic moment on these impurities are now well known in the dilute limit, it seems reasonable to use the $\delta_0$ parameter that yields the experimental values, namely, 1.6 $\mu_B$, 2.6 $\mu_B$, and 3.5 $\mu_B$ on Co,[30] Fe,[31] and Mn,[32] respectively. For the *Ni*Co and *Ni*Fe alloys this determination corresponds to fulfill the Friedel sum rule for the $\delta_\sigma$ parameters in the dilute limit:

$$Z = \sum_\sigma \frac{5}{\pi} \frac{\delta_\sigma \operatorname{Im} F_\sigma(E_F)}{1 - \delta_\sigma \operatorname{Re} F_\sigma(E_F)}, \tag{3}$$

as given by Clogston,[33] where $Z$ is the excess of charge in the matrix.

### C. Results

As it has been already shown, the expression of the energy in the Hartree-Fock approximation leads to several solutions. We have shown in Fig. 2 the variation of the magnetic moment with $Z$. This curve is similar to that obtained in previous works[5,6] if we take into account some differences between the set of parameters. Each line segment corresponds to a type of solution with specific characteristics. There is one solution or three solutions depending on the $Z$ value. This multiplicity is not related to the $\Sigma_\sigma(z)$ determination (obtained in a unique way by using its limit at $z$ infinite), but, as explained by Kanamori,[34] is a consequence of the analytical form of the Hartree-Fock energy.

We have shown in Fig. 3 the schematic partial densities of states $n_{\alpha,\sigma}(E)$ ($\alpha = A, B$; $\sigma = \uparrow, \downarrow$) corresponding to each solution. The arrows indicate the evolution of the deformation on the impurity site at small concentration when $Z$ is increasing. Of course, this evolution is directly related to that of the sign and magnitude of the self-consistent $\delta_\sigma$ parameters; in particular, the partial den-

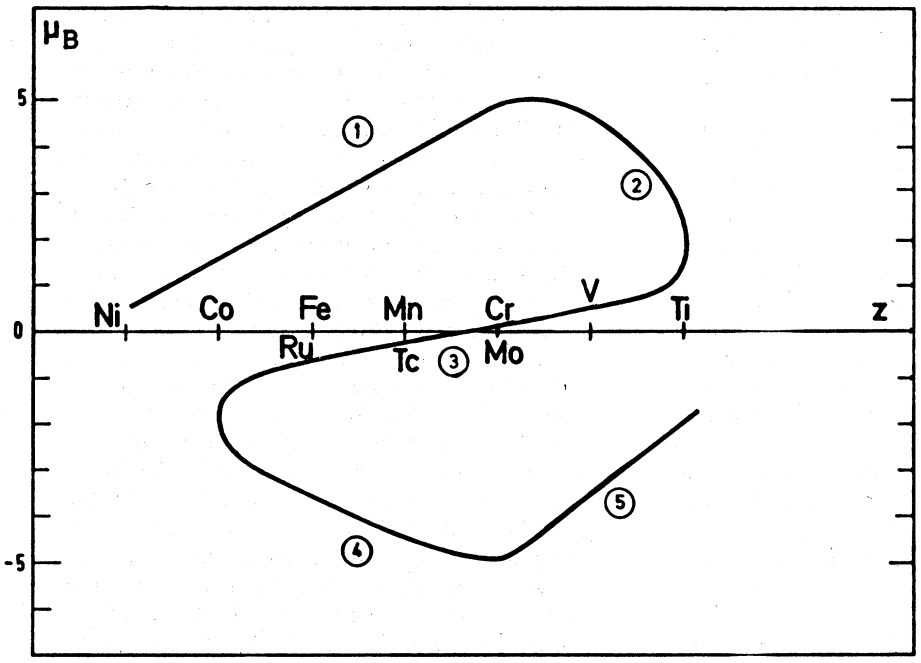


FIG. 2. Solutions of the Hartree-Fock equation for impurities in nickel. Magnetic moment of the impurity vs its excess of charge $Z$ in the matrix.

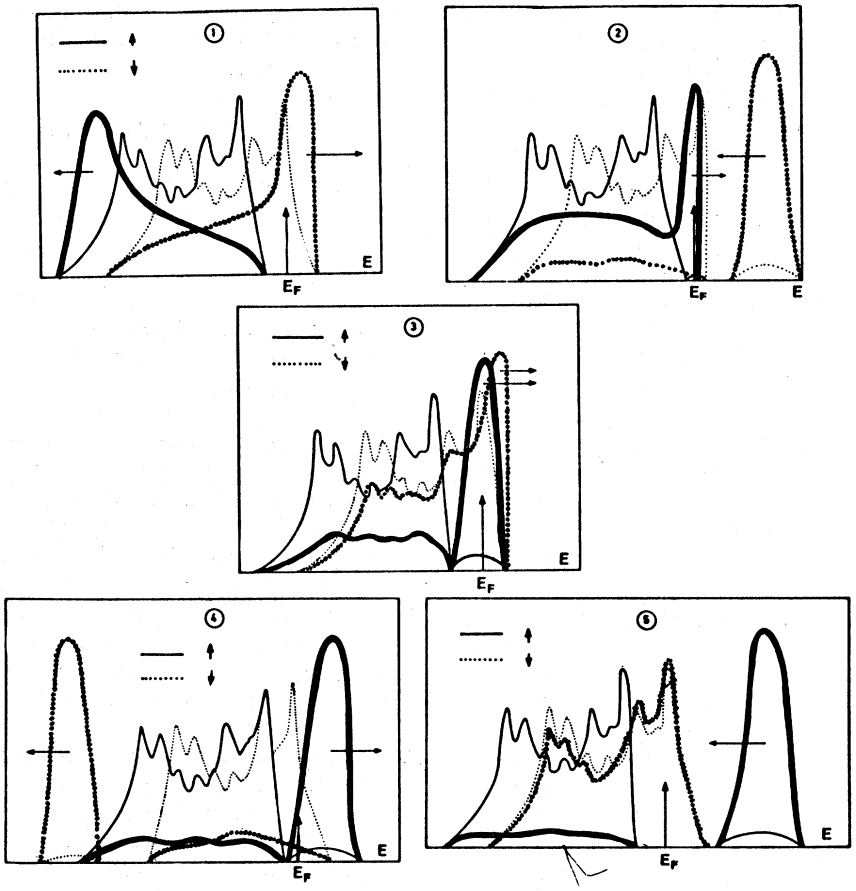


FIG. 3. Schematic partial densities of states in each solution: Solid line $n_{A\uparrow}(E)$; bold solid line, $n_{B\uparrow}(E)$; dotted line, $n_{A\downarrow}(E)$; bold dotted line, $n_{B\downarrow}(E)$. The arrows indicate the displacement of the bound levels when $Z$ is increasing at small impurity concentration.

sities of states may exhibit bound states when the $\delta_\sigma$ values go beyond some critical values which are functions of the band shape. The variation of the magnetic moment on the impurity,

$$m_B = \int_{-\infty}^{E_F} [n_{B\uparrow}(E) - n_{B\downarrow}(E)]\, dE ,$$

with $Z$ is easily predicted from these schemes by considering the change in the deformation of $n_{B\sigma}(E)$ with $Z$.

Let us now comment briefly on the different solutions. Indeed we have to follow their evolution with $Z$ at fixed concentration, which is a consequence of the Hartree-Fock approximations and their evolution with the concentration at fixed $Z$, which, in its turn, is a consequence of the coherent-potential approximation. This will allow us to make assumptions on the physical description of the behavior of the various alloys and to compare these to interpretations given in previous papers.

*Solution* (i): $\delta\uparrow$ is negative and $\delta\downarrow$ is positive. Then the deformations occur at the bottom of $n_{B\uparrow}(E)$ and the top of $n_{B\downarrow}(E)$. Both increase with $Z$ in magnitude. Accordingly, $n_{B\uparrow}(E)$ is always full, while $n_{B\downarrow}(E)$ is progressively emptied as $Z$ is increased, which corresponds to the increase of the magnetic moment on the impurity $B$ atom.

When varying the impurity concentration, the main characteristics of the solution are (a) The alloy remains a strong ferromagnet and no magnetic transition occurs. (b) The magnetization increases with concentration. (c) The stiffness constant decreases. We shall give more details below since this solution gives a good description of *Ni*Co, *Ni*Fe, and *Ni*Mn, at least in some range of concentration.

*Solution* (ii): $\delta\uparrow$ is small and $\delta\downarrow$ is large and positive. The former increases with $Z$, while the latter decreases as indicated by the arrows in Fig. 3. When $Z$ is increasing, an up bound level is progressively subtracted from the $\uparrow$ main band and emptied by crossing the Fermi level, which explains the decrease of the magnetic moment on the impurity.

When the impurity concentration is varying at a fixed $Z$ value, the characteristics are similar to those of solution (i); the magnetic moment remains nearly constant at all concentrations and $D$ decreases.

*Solution* (iii): The $\delta_\sigma$ parameters are positive and determine a small magnetic moment on the impurity, increasing with $Z$. $\delta_\uparrow$ is large enough to create an up bound state. With change in impurity concentration, the model predicts a transition to the paramagnetic state and a decrease of the $D$ constant and of the magnetization. We shall examine in more detail this solution since it gives a plausible description of alloys such as *Ni*Cr, *Ni*V, *Ni*Mo, and *Ni*Ru.

*Solution* (iv): $\delta_\uparrow$ is positive and $\delta_\downarrow$ is negative. Both increase in magnitude with $Z$. Because of the nearly empty up bound state, the magnetic moment is negative on the impurity and decreases as $n_{B\uparrow}(E)$ is progressively emptied as indicated by the arrow.

The variations of the partial or total magnetizations and of the stiffness constant are reproduced in Fig. 4 in the case of one alloy, with the corresponding densities of states. The magnetic moments on the atoms remain nearly constant with the concentration, and the total magnetization

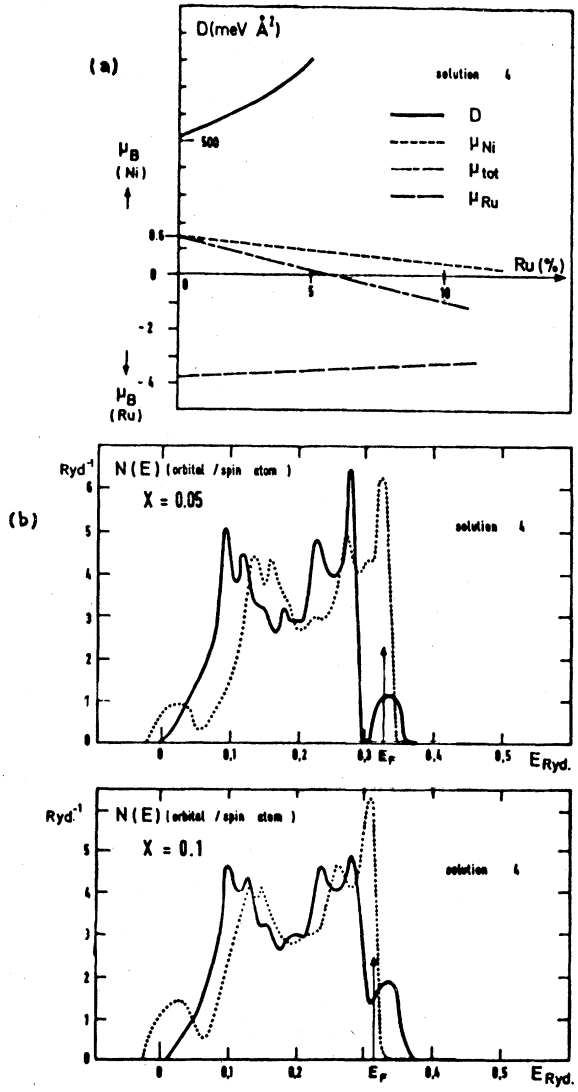


FIG. 4. (a) Variation of the partial and total magnetizations and of the stiffness constant with impurity concentration in the Hartree-Fock solution (iv). The set of parameters correspond to the *Ni* Ru case. (b) Corresponding density of states at 5% and 10% Ru.

quickly decreases. At some concentration the latter crosses the zero value leading to an unphysical situation. On the other hand, the constant $D$ increases with concentration in relation with the occurrence of a large negative moment on the impurity. It increases slightly when the impurity has $-3\mu_B$ moment value and more strongly for larger negative values.

*Solution* (v): $\delta_\uparrow$ is much larger than $\delta_\downarrow$, and both have opposite variations when $Z$ increases. Results for the magnetization and the stiffness-constant variation with the impurity concentration are shown in Fig. 5, in one case of alloy with the corresponding density of states. As in solution (iv), the total magnetization decreases while the stiffness constant strongly increases.

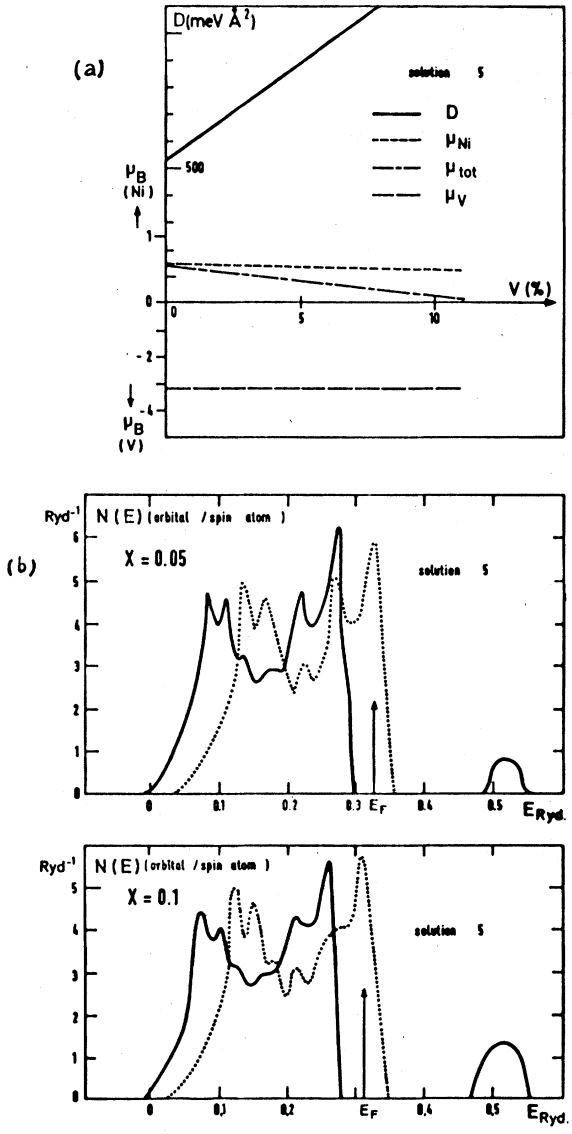


FIG. 5. (a) Variation of the partial and total magnetizations and of the stiffness constant with impurity concentration in the Hartree-Fock solution (V). The set of parameters correspond to the *Ni*V case. (b) Corresponding density of states at 5% and 10% V.

The comparison between the experimental behavior of magnetic moments and of the stiffness constant, leads us to conclude that solution (i) describes the *Ni*Co, *Ni*Fe, and *Ni*Mn alloys because of the good agreement of the calculated magnetic-moment value on impurity with those obtained by neutron experiments. This conclusion has already been reached in several previous works.[1,2,4] On the other hand, solution (iii) may be thought to describe the alloys, the magnetizations of which deviate from the Slater-Pauling curve. However, this does not agree with previous theoretical works[1,2] which usually have considered solution (v) to describe this category of alloys.

Our conclusion is based on comparison with three main experimental results: First, solution (iii) predicts a small moment on the impurity instead of a large negative moment, as in solutions (iv) or (v). This is in rather good agreement with the results of diffuse neutron scattering.[35,36] Second, $D$ decreases with concentration as observed experimentally, while it increases in solutions with a large negative moment. Third, at larger concentrations the model predicts a paramagnetic transition, while in other solutions no magnetic transition occurs. Of course this last argument can be questioned, since the CPA is not expected to describe correctly a magnetic transition.

One of the main objections to our inference is that it is not supported by some energy calculations. Indeed, it has been found[6] that both Hartree-Fock solutions with a large positive or negative magnetic-moment values are stable, while the third with a small moment value is not. However, it seems to us that theoretical considerations of the stability of electronic states should take into account the complexity of the atomic electronic orbitals and of the local atomic environment. Accordingly, we think that these results are important but cannot constitute a definitive argument, and it would be of great interest to perform further calculations to clarify this problem.

## III. LIMITS OF THE MODEL

In this section we compare in more details results of the model with experiments in the two chosen solutions.

### A. *Ni*Co, *Ni*Fe, and *Ni*Mn

In Fig. 6 we have shown $D$ measurements obtained by inelastic neutron scattering and its calculated variations obtained in solution (i) with the parameters corresponding to *Ni*Co, *Ni*Fe, and

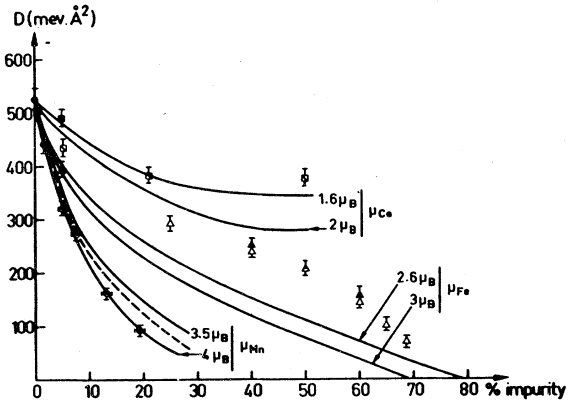


FIG. 6. ——, variations of $D$ with impurity concentration in the CPA-RPA model. Comparison with experiments: $Ni$Co = ■ (4.2 K), □ (293 K); $Ni$Fe = ▲ (4.2 K), △ (293 K); $Ni$Mn = ● (4.2 K). For each alloy, two calculations have been performed, corresponding to two different calculated values of the magnetic moment on the impurity. These values are indicated in the graphs, ------, $D$ variation of $Ni$Mn in the ternary model (see Figs 8 and 9).

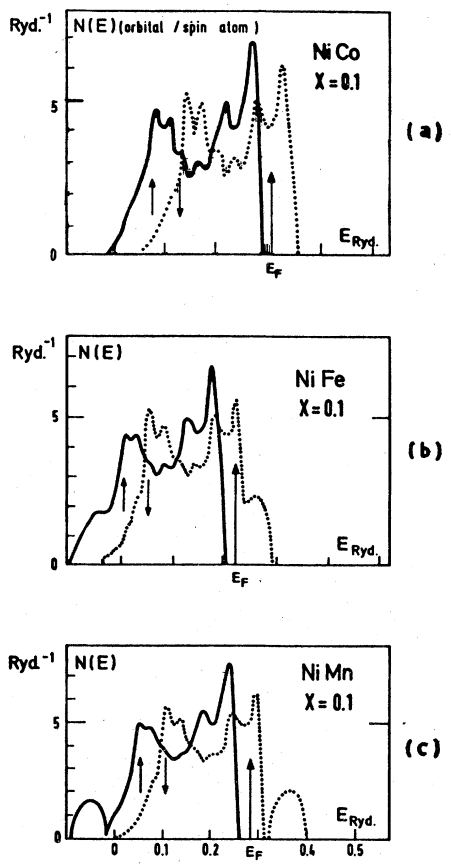


FIG. 7. Density of states of $Ni$Co (a), $Ni$Fe (b), and $Ni$Mn (c) at 10% of impurity concentration: ——, up band; ···, down band. The Fermi level is indicated by $E_F$. The origin of energies is arbitrary.

$Ni$Mn alloys. For simplification, we have not included the experimental results of other authors[37-39] that have already been compared in previous works. The total density of states of the three alloys at 5% concentration are shown in Fig. 7.

Keeping in mind all the approximations used, the model accounts satisfactorily for the qualitative features of the $D$ variation, both with the concentration and the $Z$ value of the impurity. (The case of $Ni$Fe has already been reported.[14]) The sensitivity of the calculated stiffness constant to a variation of the parameters is shown in the same figure, where are plotted two curves $D(c)$ corresponding to two different values of the magnetic moment on the impurity.

However, the model cannot account for the large bump observed in $Ni$Fe at about 50% Fe. It may be invoked that the $U^{\text{eff}}$ values have to vary with concentration. Anyway, the peculiar behavior of $D$ in this alloy has obviously to be related to the rapid decrease of the experimental magnetization beyond 50% Fe which does not occur in the model.

Indeed, the limits of the model appear more clearly if we look at the magnetization variation. The calculated magnetizations which correspond to a simple integration of the band up to the Fermi level give the same results as does the rigid-band model; it cannot predict any decrease in $Ni$Fe and $Ni$Mn. This discrepancy may lead one to question the agreement found for the $D$ variation, especially in the $Ni$Mn case, where it occurs as early as 10% of Mn.

We can recall that the decrease of the magnetization in these alloys has been attributed to the entry of the Fermi level in the up band in the pioneering work of Hasegawa and Kanamori.[4] This was a consequence of the small-$U$ value used by these authors. It is more usually thought now that this decrease is, rather, related to local-environment effects, which may induce a change of the electronic state of the impurity. Indeed, by performing an energy calculation, Jo[40] has shown that Mn atoms may coexist in two different electronic states with opposite magnetic moments depending on the Mn concentration. These states correspond to solutions (i) and (iv) in the general curve (Fig. 2). It is then of interest to examine the consequences of these antiferromagnetic states on the calculated stiffness-constant behavior.

Such a possibility may be introduced in a phenomenological ternary model $Ni_{1-x}Mn_y^{I}Mn_z^{II}$, where the ratio of $Mn^{I}$ and $Mn^{II}$ atoms is arbitrarily fixed by a probability law. Following an assumption given by other authors,[41,43] a Mn atom will have a negative moment when surrounded by more than

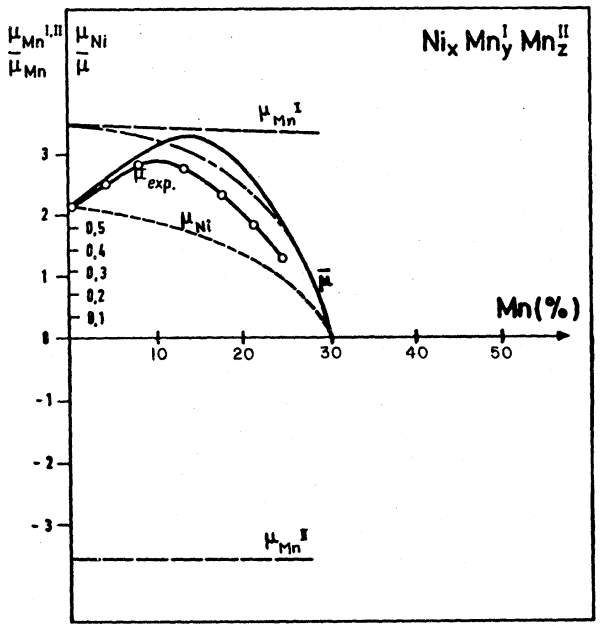


FIG. 8. Magnetization variations with Mn concentration in the ternary model: — —, calculated magnetizations variations on $Mn^I$ and $Mn^{II}$ atoms ($\mu_{Mn}^{I,II}$); -----, calculated magnetizations variations on Ni atoms ($\mu_{Ni}$); – – –, mean magnetization on Mn atoms ($\bar{\mu}_{mn}$); ——, total calculated magnetization ($\bar{\mu}$); -o-o-o, total experimental magnetization ($\bar{\mu}_{exp}$).

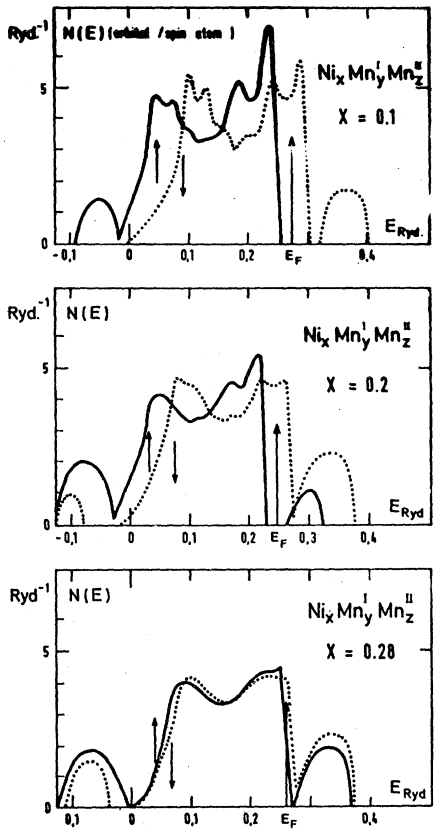


FIG. 9. Density of states of *Ni*Mn in the ternary model.

three Mn atoms, regardless of their states. In this ternary model, the self-energy $\Sigma_\sigma(z)$ of the effective medium is determined by Eq. (2), where the summation is extended to the three types of sites.

Results for magnetizations and stiffness constants are shown in Figs. 8 and 7, with the corresponding densities of states in Figure 9.

In this model, the magnetic moment on Mn atoms keeps a nearly constant value while the nickel atoms go to the paramagnetic state near 30% Mn. At that concentration, the alloy may be considered to be in a disordered antiferromagnetic state. The calculated magnetization curve agrees qualitatively with the experimental curve. The probability law is, of course, oversimplified. Nevertheless, the model can show that the stiffness constant is hardly affected by the antiferromagnetic states of some Mn atoms.

Such a model could approximately reproduce the decrease of magnetization in *Ni*Fe alloys, too, with an appropriate probability law to define the relative $Fe^I$ and $Fe^{II}$ atom concentrations, but it cannot account for the peculiar behavior of the stiffness constant. In this alloy, $D$ seems rather sensitive to the complexity of the local perturbation where clustering and ordering effects have been revealed by neutron experiments, and it is clear that all the mean-field approximations such as RPA or CPA in ternary- as well as in binary-alloy models are no longer sufficient.

### B. *Ni*V, *Ni*Cr, *Ni*Mo, and *Ni*Ru

Results obtained in solution (iii) with parameters corresponding to *Ni*V, *Ni*Cr, *Ni*Mo, and *Ni*Ru are plotted on Figs. 10 and 11, and compared to the experimental results. It appears then that the stiffness constant and the magnetization have similar variation with impurity concentration, as it has been observed experimentally. The alloys come progressively to the paramagnetic state, and the calculated critical concentrations have the same order of magnitude as in the experiments.

Densities of states of *Ni*Ru and *Ni*Cr are reproduced in Fig. 12. At small concentration, they exhibit an up-band level half filled in the *Ni*Ru case and nearly empty in *Ni*Cr (or *Ni*V and *Ni*Mo). The decrease of the magnetization with impurity concentration is related to the occurrence of the empty up states which induce an electron transfer from the up band to the Fermi level in the down band, and then a change of polarity, as qualitatively explained by Friedel.[3] The evolution of the magnetization decrease with the change of impurity

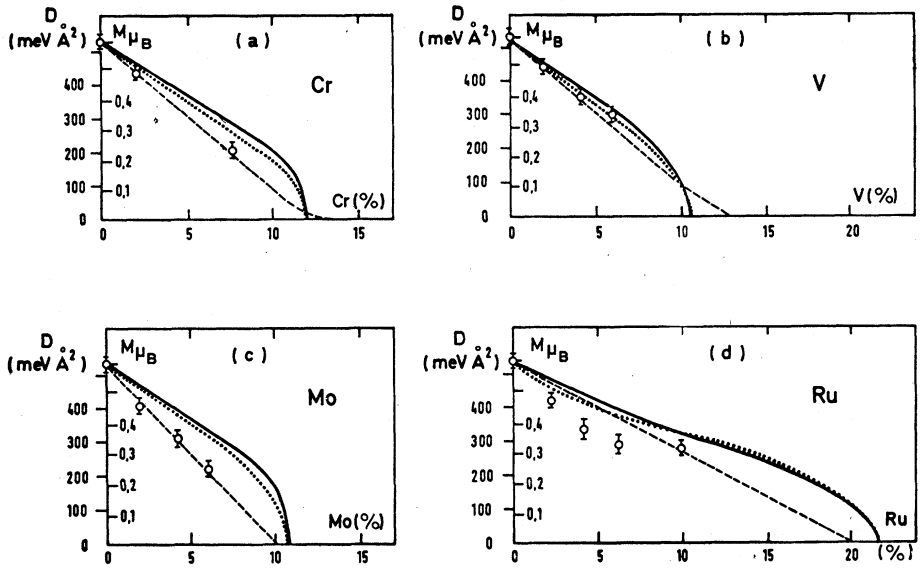


FIG. 10. Comparison between calculation and experiment for the concentration dependence of magnetization and stiffness constant in *Ni*Cr (a), *Ni*V (b), *Ni*Mo (c), and *Ni*Ru (d); ——, calculated magnetization; ····· calculated stiffness constant; ----, magnetization measurement. ⊼, stiffness-constant measurement (Ref. 9).

(for instance, from Ru to Mo) is explained by the corresponding evolution of the empty up states of the total densities of states with the impurity, as shown in Fig. 12.

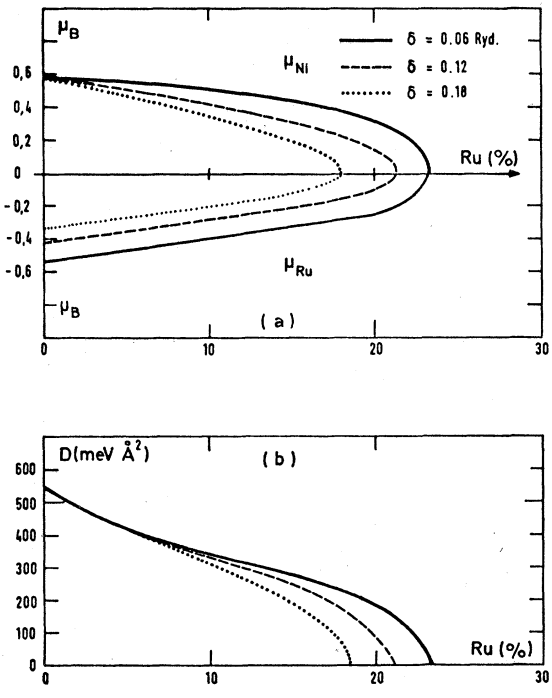


FIG. 11. Sensitivity of the calculated parameters to a change in the parameter δ in the *Ni*Ru case [solution (iii)]: ——, δ = 0.06 Ry; -----, δ = 0.12 Ry; ·····, δ = 0.18 Ry. The value δ = 0.12 Ry corresponds to the ruthenium (Fig. 1) impurity; the values δ = 0.06 Ry and δ = 0.18 correspond to the neighboring elements in the variation of Fig. 1.

We have to note, however, that the deviation from the linearity of the $D(c)$ curve observed experimentally in the *Ni*Ru case is not well accounted for by the model. It may be thought that the situation is more complex at small Ru concentration, and this can be in relation with other peculiarities observed in this alloy.

In fact, the agreement is more qualitative than quantitative. It may be objected indeed that solution (v) gives a better $d\mu/dc$ value ($\mu$ being the mean magnetization) than in solution (iii), where this parameter is too small. But this can be explained since the single-site approximation neglects the environment effects and then is unsuited in the dilute limit. Accordingly, the model has to be checked for the overall results on a rather large range of concentrations, especially in this category of alloys where the perturbation is known to be extended in real space.

The extension of the perturbation can be understood in this solution since the scattering potentials $\delta_\sigma$ obtained in the dilute limit largely disagree with the Friedel sum rule. These parameters cannot conciliate Eq. (3) with the requirement that the screening is effective on the impurity atom. This large perturbation can explain the high resistivity measured in this category of alloys, since a great deal of perturbed atoms surrounding the impurity may scatter the electrons.

Near the critical concentration the calculated $D$ and $M$ variations become nearly parabolic. It would be exactly parabolic if $m_A = m_B$. We can note that this single-site model gives the same result as does the theory of Mathon[42] or Edwards and Wohlfarth,[43] which uses the Landau equations for the second-order phase transition. Indeed,

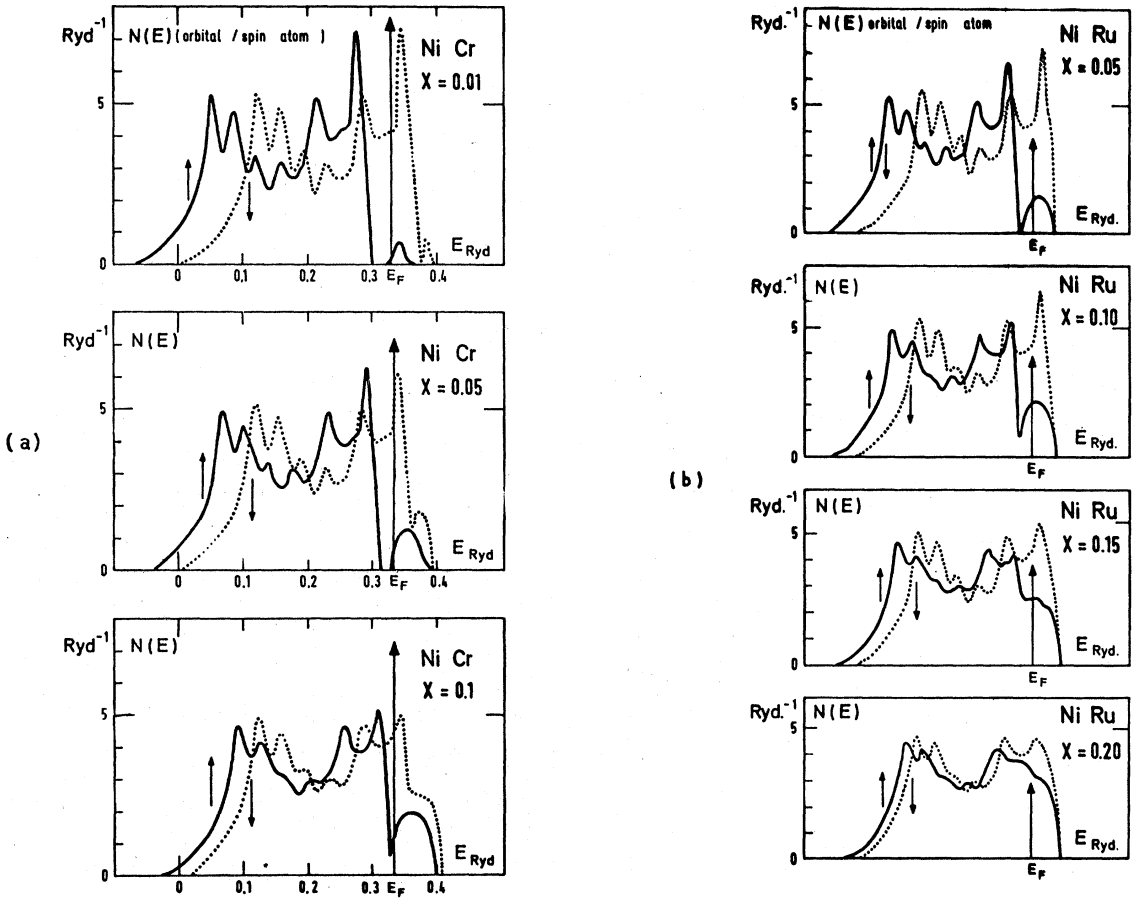


FIG. 12. (a) Density of states of *Ni* Cr at 1%, 5%, and 10% Cr (in $Ry^{-1}$ per atomic orbital and per spin); (b) Density of states of *Ni*Ru at 5%, 10%, 15%, and 20% Ru. —, up band; · · · · ·, down band.

this last theory can predict a parabolic variation of $D$ and $M$ near the magnetic transition for weak and homogeneous alloys. This behavior is not found experimentally in these alloys, where experiments have revealed magnetic clusters, but it has been observed in some alloys like *Ni*Pt expected to be homogeneous in the critical region. Of course, the parabolic behavior should not occur in a more improved model ($n$-site CPA) which takes into account the local environments.

## IV. SUMMARY AND CONCLUSION

By performing experimental measurements of the stiffness constant in several nickel alloys and giving a theoretical description of the possible impurity states in the Hartree-Fock approximation, we have tried to clarify the microscopic electronic structure of the nickel-based alloys. Indeed, we have found that a RPA-CPA model can give a rather satisfactory description of the $D$ constant in these alloys under the following conditions:

(a) One uses a rather large value for the intra-atomic interaction parameter of nickel (0.5 Ry) considered here as an effective parameter of the model. In spite of the sensitivity of $D$ to this parameter, we think that our comparison is meaningful since it is extended to several Ni alloys.

(b) One describes the alloys in two Hartree-Fock solutions depending on the type of impurity; in particular, for the impurities Cr, V, Ru, and Mo we assume that these alloys are described in a solution that determines a small magnetic moment on the impurity.

Within these assumptions and for each category of alloys, we could then discuss the limits of the model. They appear to be mainly due to local environment effects.

Although the choice of the Hartree-Fock solutions seems supported up to now by several experimental results, it could be checked further as, for instance, in the *Ni*Ru case by direct measurement of the magnetic moment of Ru. The main objection to the chosen description for this category of alloys comes from theoretical considerations on the stability of the electronic states, and

it would be of interest to investigate this point by further calculations.


## ACKNOWLEDGMENTS

The authors are very indebted to Dr. M. Nauciel-Bloch and Dr. R. Riedinger for enlightening comments on their initial work. They would also like to thank Professor J. Friedel, Professor F. Gautier, and Professor I. A. Campbell for fruitful discussions and suggestions.


## APPENDIX

The parameters $N_{\alpha,\sigma}$ and $E_F$ are determined self-consistently as follows.

First, we build a function of these parameters:

$$\mathfrak{F}(N_{\alpha,\sigma}, E_F) = \sum_{\alpha,\sigma} [N_{\alpha,\sigma} - f_{\alpha,\sigma}(\Sigma_\sigma, E_F)]^2 + \left[ N(x) - \sum_{\alpha,\sigma} x_\alpha f_{\alpha,\sigma}(\Sigma_\sigma, E_F) \right]^2 ,$$

$$\alpha = A, B, \quad \sigma = \uparrow, \downarrow$$

where the $f_{\alpha,\sigma}(\Sigma_\sigma, E_F)$ are the analytical expressions of $N_{\alpha,\sigma}$,

$$f_{\alpha,\sigma} = -\frac{1}{\pi} \int_{-\infty}^{E_F} \mathrm{Im} F_{\alpha,\sigma}(E^+)\, dE ,$$

or, equivalently, by use of the Cauchy theorem

$$f_{\alpha,\sigma} = \frac{1}{2} + \frac{1}{\pi} \int_0^\infty \mathrm{Re} F_{\alpha,\sigma}(E_F + iy)\, dy ;$$

the latter expression facilitates the numerical calculation because outside the real axis $F(z)$ is a smooth function of $z$.

For each $z$ $(z = E + iy)$, $\Sigma_\sigma(z)$ is obtained by an iterative procedure

$$\Sigma_\sigma^i = \Sigma_\sigma^{i-1} + \frac{\langle t_{\alpha,\sigma}^{i-1} \rangle}{1 + \langle t_{\alpha,\sigma}^{i-1} \rangle F(z - \Sigma_\sigma^{i-1})} ,$$

with

$$\langle t_{\alpha,\sigma}^{i-1} \rangle = \sum_\alpha x_\alpha \frac{\epsilon_{\alpha,\sigma} - \Sigma_\sigma^{i-1}}{1 - (\epsilon_{\alpha,\sigma} - \Sigma_\sigma^{i-1}) F(z - \Sigma_\sigma^{i-1})} .$$

Then we look for the minimum of this function. Indeed, it will reach its minimum value, zero, when the set of equations will be satisfied. The determination of the minimum is made by use of the iterative descent method of Davidon in the simplified version due to Fletcher and Powell.[19] This method needs the analytical first derivatives of the function. It consists in locating at each step a minimum along a line. Starting from the steepest descent, the choice of the line at successive iterations is improved by calculating an approximation of the matrix inverse of that of the second derivatives. This procedure allows a quadratic convergence and yields the curvature of the function at the minimum, providing excellent tests for convergence and estimates of variance.


[1] I. A. Campbell and A. A. Gomes, Proc. Phys. Soc. 91, 319 (1967).
[2] C. Demangeat and F. Gautier, J. Phys. C. Suppl. 3, 529 (1970); Met. Phys. 3, S 291 (1970).
[3] J. Friedel, Nuovo Cimento 7, 287 (1958).
[4] H. Hasegawa and J. Kanamori, J. Phys. Soc. Jpn. 31, 382 (1971); 33, 1599 (1972).
[5] H. Hayakawa and J. Yamashita, Prog. Theor. Phys. 54, 952 (1975).
[6] T. Jo and H. Miwa, J. Phys. Soc. Jpn. 40, 706 (1976).
[7] M. Hennion, B. Hennion, A. Castets, and D. Tocchetti, Solid State Commun. 17, 899 (1975).
[8] B. Hennion, M. Hennion, and F. Kajzar, in *Proceedings of IAEA* (IAEA, Vienna, 1978).
[9] M. Hennion, and B. Hennion, J. Phys. F 8, 287 (1978).
[10] B. Hennion and M. Hennion, J. Phys F (to be published).
[11] H. Fukuyama, *Proceedings of the Conference on Magnetism and Magnetic Materials*, edited by C. D. Graham and J. J. Rhyne (AIP, N. Y., 1973), p. 1727.
[12] D. J. Hill and D. M. Edwards, J. Phys. F 3, 162 (1973).
[13] M. Nauciel-Bloch and J. Riedinger, Phys. F 4, 1032 (1974).
[14] R. Riedinger and M. Nauciel-Bloch, J. Phys. F 5, 732 (1975).
[15] P. Soven, Phys. Rev. 97, 304 (1967).
[16] B. Velicky, S. Kirkpatrick, and H. Ehrenreich, Phys. Rev. 175, 747 (1965).
[17] R. Fletcher and M. J. D. Powel, Comp. J. G-ESS 2, 163 (1963); W. C. Davidon, EEC Research and Development Report No. ANL 5990 (Rev), 1959 (unpublished).
[18] S. J. Wakoh, Phys. Soc. Jpn. 30, 1068 (1971).
[19] G. C. Fletcher, Proc. R. Soc. Lond. 65, 192 (1952). Of course, this band structure is not quite elaborate and, for instance, disregards the *s-d* hybridization usually accounted for in more actual calculations. Nevertheless, in regard of all the other approximations of the model it may be thought realistic enough, and we used it for sake of simplicity.
[20] H. A. Mook, J. W. Lynn, and R. M. Nicklow, Phys. Rev. Lett. 30, 556 (1973).
[21] M. Hennion, B. Hennion, M. Nauciel-Bloch, and R. Riedinger, J. Phys. F 6, No. 11 (1976).
[22] S. Wakoh, J. Phys. Soc. Jpn. 20, 1894 (1965).
[23] L. Hodges, H. Ehrenreich, and N. D. Lang, Phys. Rev. 152, 505 (1966).
[24] J. W. D. Connolly, Phys. Rev. 159, 415 (1967).
[25] E. I. Zornberg, Phys. Rev. B 1, 244 (1970).
[26] C. S. Wang and J. Callaway, Phys. Rev. B 9, 4897 (1974).
[27] J. F. Cooke and H. L. Davis, AIP Conf. Proc. 10, 1218 (1973).
[28] G. C. Fletcher and B. A. Nudel, Int. J. Quantum Chem. Symp. 7, 619 (1973); see also B. N. Cox, M. A. Coulthard, and P. Lloyd, J. Phys. F 4, 807 (1974).
[29] F. Herman and S. Skillman, in *Atomic Structure Cal-*

*culations* (Prentice-Hall, London, 1963).
[30]M. F. Collins and D. A. Wheeler, Proc. Phys. Soc. Lond. 82, 633 (1963).
[31]C. G. Shull and M. K. Wilkinson, Phys. Rev. 97, 304 (1955); M. F. Collins, R. V. Jones, and R. D. J. Lowde, Phys. Soc. Jpn. 17, 19 (1962).
[32]J. W. Cable and H. R. Child, Phys. Rev. B 10, 4607 (1974).
[33]A. M. Clogston, Phys. Rev. 125, 439 (1962).
[34]J. Kanamori, J. Phys. 35, 137 (1974).
[35]J. W. Cable and R. A. Medina, Phys. Rev. B 13, 4868 (1976).
[36]F. Livet and P. J. Radakrishna, Phys. Chem. Solids 38, 275 (1977).
[37]K. Mikke, J. Jankowska, A. Modrzejewski, and E. Frikke, Physica 86–88 (B+C), 345 (1977).
ence on Magnetism, Amsterdam (1976) (unpublished).
[38]K. Mikke, J. Jankowska, and A. Modrzejewski, J. Phys. F 6, 631 (1976).
[39]A. Z. Menshikov, V. A. Kazantsev, N. N. Kusmin, and S. K. Sidorov, J. Magn. Magn. Mat. 1, 91 (1975).
[40]T. J. Jo, Phys. Soc. Jpn. 40, 715 (1976).
[41]R. L. Streever, Phys. Rev. 173, 591 (1968).
[42]J. Mathon, Proc. R. Soc. Lond. 306, 355 (1968).
[43]D. M. Edwards and E. P. Wohlfarth, Proc. R. Soc. Lond. 303, 127 (1968).